# Joint Input and Output Channel Selection for Multi-channel Feedforward Active Noise Control

1st Yanrong He
*College of Computer Science*
*Inner Mongolia University*
Hohhot, China
yrhe@mail.imu.edu.cn

2nd De Hu*
*College of Computer Science*
*Inner Mongolia University*
Hohhot, China
cshood@imu.edu.cn

***Abstract*—By using multiple reference microphones as input channels and multiple loudspeakers as output channels, multi-channel feedforward active noise control (ANC) systems can achieve better noise reduction performance compared to single-channel feedforward ANC systems. However, as the number of channels increases, the computational load rises significantly, affecting the system's real-time capability. In this work, a joint input and output channel selection (J-IO-CS) method is proposed for multi-channel feedforward ANC to improve its computational efficiency. We first design a novel channel selection model by minimizing the residual noise power while constraining computational complexity through the group sparsity of spatial filters. Due to the non-convex nature of the above model, we convert it into a convex problem via the $\ell_{1,2}$-norm after exchanging its objective and constraint. Furthermore, we introduce an adjustable parameter to ensure that the reformulated problem is equivalent to the original one. To the best of our knowledge, the proposed J-IO-CS method is the first attempt to simultaneously select input and output channels in multi-channel feedforward ANC systems, which delivers higher computational efficiency than existing input channel selection approaches. Numerical experiments confirm its validity.**

***Index Terms*—multi-channel active noise control, feedforward control, convex optimization, channel selection.**

## I. Introduction

Active noise control (ANC) has garnered significant attention in various applications, such as headphones [1], headrests [2], and vehicles [3], among others. The traditional single-channel feedforward ANC system uses a reference microphone (RM), i.e., an input channel, to capture the noise signal, then the ANC controller generates "antinoise" through a loudspeaker, i.e., an output channel, to cancel the noise at the control point [4], [5]. Since the single-channel feedforward ANC system utilizes only one input channel and one output channel, its performance is often limited in complicated noise environments [6].

To cope with more complex noise scenarios, multi-channel feedforward ANC systems adopt multiple RMs and multiple loudspeakers, resulting in significantly improved noise reduction performance [7], [8]. Theoretical analysis and experimental results show that the more input or output channels, the better the ANC performance [9]. However, increasing both the number of input and output channels simultaneously raises computational complexity quadratically [10], [11], which may affect the system's real-time capability.

Modifications can be made to the multi-channel feedforward ANC configuration to reduce computational complexity. For example, the co-located ANC structure ignored cross-reference effects, which can reduce the number of redundant spatial filters to save computational resources [12]. Another strategy is to reduce computational load by selecting the most informative subset of RMs. In [13], the time difference of arrival (TDOA) between the RM and the error microphone (EM) was first estimated, and then the RM that satisfies causality was selected. Recently, Zhang *et al.* analyzed the impact of the coherence between RM signals and EM signals on the multi-channel feedforward ANC system [14]. Based on that, high-coherence RMs were selected to conduct noise control in [15]. However, the studies above only reduced redundancy within the input channels (i.e., RMs) while ignoring the redundancy in output channels (i.e., loudspeakers).

In this paper, to further improve computational efficiency, we propose a joint input and output channel selection (J-IO-CS) method for multi-channel feedforward ANC systems. Specifically, the best subset of input and output channels is defined by minimizing the residual noise power under a pre-specified computational complexity constraint. As the above criterion involves non-convex programming, we convert it into a convex one by introducing an adjustable parameter $\alpha$. By finding an appropriate value for $\alpha$, we can obtain a near-optimal channel selection result. Compared with existing methods, the J-IO-CS method shows better performance in terms of computational efficiency.

## II. Fundamental

### A. Multi-channel Feedforward ANC System

Let us consider a general $(I, J, K)$ multi-channel feedforward ANC system (Fig. 1), where the ANC controller receives the noise signals that are captured by $I$ RMs, and emits "anti-noise" through $J$ loudspeakers to cancel the noises at $K$ control points. The control signal $y_j(n)$ emitted by the $j$-th

*: Corresponding Author. This work was supported by the National Natural Science Foundation of China under Grants 62361045 and 62201297.

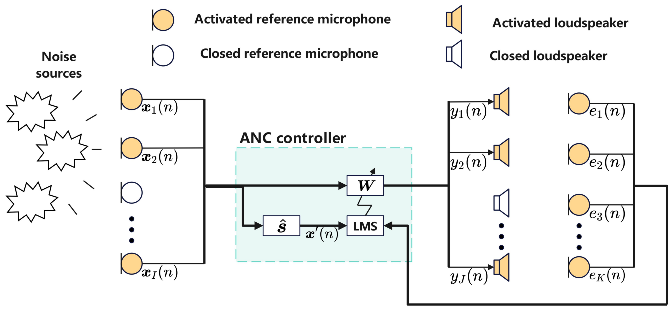


Fig. 1. Block diagram of the multi-channel feedforward ANC system.

loudspeaker at time $n$ can be expressed as

$$y_j(n) = \sum_{i=1}^{I} \boldsymbol{x}_i^{\mathrm{T}}(n)\boldsymbol{w}_{ji}(n), \tag{1}$$

where superscript $(\cdot)^{\mathrm{T}}$ indicates the matrix (or vector) transpose, $\boldsymbol{x}_i(n) = [x_i(n), x_i(n-1), ..., x_i(n-M+1)]^{\mathrm{T}}$ with $x_i(n)$ denoting the received signal of the $i$-th RM at time $n$, and $\boldsymbol{w}_{ji}(n) = [w_{ji,1}(n), w_{ji,2}(n), ..., w_{ji,M}(n)]^{\mathrm{T}}$ is the $M$-order noise control filter that is related to RM $i$ and loudspeaker $j$. An EM is placed at the $k$-th control point to record the residual noise signal $e_k(n)$, which can be expressed as

$$e_k(n) = d_k(n) + \sum_{j=1}^{J} \boldsymbol{y}_j^{\mathrm{T}}(n)\boldsymbol{s}_{kj}, \tag{2}$$

where $\boldsymbol{y}_j(n) = [y_j(n), y_j(n-1), ..., y_j(n-L+1)]^{\mathrm{T}}$, $d_k(n)$ represents the unwanted noise (i.e., desired signal) captured by the $k$-th EM at time $n$, and the secondary path between the $k$-th EM and the $j$-th loudspeaker is modeled as an $L$-tap FIR filter $\boldsymbol{s}_{kj} = [s_{kj}(0), s_{kj}(1), ..., s_{kj}(L-1)]^{\mathrm{T}}$. According to (2), the unwanted noise at the $k$-th EM can be estimated as

$$\hat{d}_k(n) = e_k(n) - \sum_{j=1}^{J} \boldsymbol{y}_j^{\mathrm{T}}(n)\hat{\boldsymbol{s}}_{kj}, \tag{3}$$

where $\hat{d}_k(n)$ is the estimate of $d_k(n)$, and $\hat{\boldsymbol{s}}_{kj}$ is the estimate of $\boldsymbol{s}_{kj}$, which can be obtained through offline modeling [16].

The goal of the multi-channel feedforward ANC is to minimize the error signals at all control points simultaneously. To achieve this, the ANC controller is required to minimize the following cost function

$$\mathcal{J} = \sum_{k=1}^{K} \mathcal{J}_k = \mathbb{E}\left\{\sum_{k=1}^{K} e_k^2(n)\right\}, \mathcal{J}_k = \mathbb{E}\left\{e_k^2(n)\right\}, \tag{4}$$

where $\mathbb{E}\{\cdot\}$ denotes the expectation operator. To meet the real-time requirements, the multiple error filtered-x least mean square (MEFxLMS) algorithm [17] adopts the instantaneous error $\sum_{k=1}^{K} e_k^2(n)$ to replace $\mathbb{E}\left\{\sum_{k=1}^{K} e_k^2(n)\right\}$ in (4), thereby obtaining the following recursive solution

$$\boldsymbol{w}_{ji}(n+1) = \boldsymbol{w}_{ji}(n) + \mu \sum_{k=1}^{K} \boldsymbol{x}'_{kji}(n)e_k(n), \tag{5}$$

where $\mu$ is the stepsize and $\boldsymbol{x}'_{kji}(n)$ is given by

$$\boldsymbol{x}'_{kji}(n) = \boldsymbol{X}_i(n)\hat{\boldsymbol{s}}_{kj}, \tag{6}$$

where $\boldsymbol{X}_i(n) = [\boldsymbol{x}_i(n)\ \boldsymbol{x}_i(n-1)\ \dots\ \boldsymbol{x}_i(n-L+1)]$. The number of multiply-accumulate operations required per iteration in the MEFxLMS algorithm is [11]

$$B = IJ(KL + KM + M) + K. \tag{7}$$

Apparently, $B$ increases quadratically with the number of input and output channels (i.e., $I$ and $J$). In other words, although a larger number of input and output channels delivers better ANC performance in the theoretical aspect, the computational complexity (i.e., $B$) increases at the same time, which may affect the real-time processing at run-time. To this end, some low-complexity multi-channel feedforward ANC algorithms were developed leveraging RM selection strategies.

### *B. Low-complexity multi-channel feedforward ANC Systems via RM Selection*

In [15], the coherence-based weight determination (CWD) algorithm was proposed to select RMs with higher utility. Specifically, let $\boldsymbol{x}_i = [x_i(1), x_i(2), ..., x_i(N)]^{\mathrm{T}}$ and $\hat{\boldsymbol{d}}_k = [\hat{d}_k(1), \hat{d}_k(2), ..., \hat{d}_k(N)]^{\mathrm{T}}$ be the $i$-th reference signal and the $k$-th estimate of the desired signal, respectively (with $N$ being the signal length in RM selection), then the coherence between $\boldsymbol{x}_i$ and $\hat{\boldsymbol{d}}_k$ can be computed as

$$C_{x_i\hat{d}_k}(\omega) = \frac{1}{S_{\hat{d}_k\hat{d}_k}(\omega)} S^*_{x_i\hat{d}_k}(\omega)\, S^{-1}_{x_ix_i}(\omega)\, S_{x_i\hat{d}_k}(\omega), \tag{8}$$

where $\omega$ represents the frequency of interest, $(\cdot)^*$ denotes the complex conjugate, $S_{x_i\hat{d}_k}(\omega)$ represents the cross-power spectral density of $\boldsymbol{x}_i$ and $\hat{\boldsymbol{d}}_k$, while $S_{x_ix_i}(\omega)$ and $S_{\hat{d}_k\hat{d}_k}(\omega)$ represent the power spectral densities of $\boldsymbol{x}_i$ and $\hat{\boldsymbol{d}}_k$, respectively. The CWD method tends to select RMs with higher $C_{x_i\hat{d}_k}$ and put other RMs to sleep.

Note that this method requires the system to be pre-trained using a small amount of observations to obtain the optimal RM subset in advance. Afterward, redundancy in RMs can be effectively reduced, achieving a linear decrease in computational complexity at the cost of light performance penalties. However, redundancy within loudspeakers still exists. Furthermore, whether the coherence between signals to evaluate the utility of RMs is truly effective remains questionable.

## III. Joint Input and Output Channel Selection (J-IO-CS) for Multi-channel Feedforward ANC

In order to simultaneously eliminate redundancy in both RMs (i.e., input channels) and loudspeakers (i.e., output channels), we propose the J-IO-CS method in this section. Similarly to (8), we conduct the proposed method from a small amount of recordings (with a length of $N$) before ANC. Then, the cost function in (4) can be equivalently written in a matrix-vector form as

$$\mathcal{J} = \hat{d} + 2\boldsymbol{w}^{\mathrm{T}}\boldsymbol{g} + \boldsymbol{w}^{\mathrm{T}}\boldsymbol{H}\boldsymbol{w}, \tag{9}$$

where

$$\hat{d} = \sum_{n=1}^{N}\sum_{k=1}^{K}\hat{d}_k^2(n), \tag{10a}$$

$$\boldsymbol{g} = \sum_{n=1}^{N}\sum_{k=1}^{K}\hat{d}_k(n)\boldsymbol{g}_k(n), \tag{10b}$$

$$\boldsymbol{H} = \sum_{n=1}^{N}\sum_{k=1}^{K}\boldsymbol{g}_k(n)\boldsymbol{g}_k^{\mathrm{T}}(n), \tag{10c}$$

$$\boldsymbol{g}_k(n) = \left[\boldsymbol{x}'^{\mathrm{T}}_{k11}(n)\ \ldots\ \boldsymbol{x}'^{\mathrm{T}}_{kJ1}(n)\ \ldots\ \boldsymbol{x}'^{\mathrm{T}}_{kJI}(n)\right]^{\mathrm{T}}, \tag{10d}$$

$$\boldsymbol{w} = [\underbrace{\boldsymbol{w}_{11}^{\mathrm{T}}\ldots\boldsymbol{w}_{J1}^{\mathrm{T}}}_{\boldsymbol{w}_1^{\mathrm{T}}}\ldots\underbrace{\boldsymbol{w}_{1i}^{\mathrm{T}}\ldots\boldsymbol{w}_{Ji}^{\mathrm{T}}}_{\boldsymbol{w}_i^{\mathrm{T}}}\ldots\underbrace{\boldsymbol{w}_{1I}^{\mathrm{T}}\ldots\boldsymbol{w}_{JI}^{\mathrm{T}}}_{\boldsymbol{w}_I^{\mathrm{T}}}]^{\mathrm{T}}, \tag{10e}$$

where $\boldsymbol{w}_{ji}$ is the time-invariant multi-channel Wiener solution and $\boldsymbol{w}_i$ is the vector containing the filter coefficients of the $i$-th input channel.

### A. Problem Modeling

Given an upper bound $B_0$ of computational load, i.e., $B \leq B_0$, this work aims to find the optimal combination of input and output channels. It can be achieved by minimizing the output noise power while constraining $B \leq B_0$, obtaining

$$\begin{aligned} \min_{\boldsymbol{w}} \quad & \hat{d} + 2\boldsymbol{w}^{\mathrm{T}}\boldsymbol{g} + \boldsymbol{w}^{\mathrm{T}}\boldsymbol{H}\boldsymbol{w} \\ \text{subject to} \quad & I_w J_w \leq \frac{B_0 - K}{K(L+M)+M}, \end{aligned} \tag{11}$$

where $I_w$ and $J_w$ indicate the numbers of input channels and output channels, respectively, and the constraint in (11) is obtained from (7) if $B \leq B_0$. Note that both $I_w$ and $J_w$ are related to the group sparsity in $\boldsymbol{w}$, which are represented as

$$\begin{aligned} I_w &= \|\boldsymbol{w}\|_{0,2} = \left\|\left[\left\|\boldsymbol{w}_1^{\mathrm{T}}\right\|_2, \left\|\boldsymbol{w}_2^{\mathrm{T}}\right\|_2, \cdots, \left\|\boldsymbol{w}_I^{\mathrm{T}}\right\|_2\right]^{\mathrm{T}}\right\|_0, \\ J_w &= \|\bar{\boldsymbol{w}}\|_{0,2} = \left\|\left[\left\|\bar{\boldsymbol{w}}_1^{\mathrm{T}}\right\|_2, \left\|\bar{\boldsymbol{w}}_2^{\mathrm{T}}\right\|_2, \cdots, \left\|\bar{\boldsymbol{w}}_J^{\mathrm{T}}\right\|_2\right]^{\mathrm{T}}\right\|_0, \end{aligned} \tag{12}$$

where $\|\cdot\|_0$ and $\|\cdot\|_2$ denote $\ell_0$-norm and $\ell_2$-norm, respectively, $\|\cdot\|_{0,2}$ denotes $\ell_{0,2}$-norm, and $\bar{\boldsymbol{w}}$ can be defined by

$$\bar{\boldsymbol{w}} = [\underbrace{\boldsymbol{w}_{11}^{\mathrm{T}}\ldots\boldsymbol{w}_{1I}^{\mathrm{T}}}_{\bar{\boldsymbol{w}}_1^{\mathrm{T}}}\ldots\underbrace{\boldsymbol{w}_{j1}^{\mathrm{T}}\ldots\boldsymbol{w}_{jI}^{\mathrm{T}}}_{\bar{\boldsymbol{w}}_j^{\mathrm{T}}}\ldots\underbrace{\boldsymbol{w}_{J1}^{\mathrm{T}}\ldots\boldsymbol{w}_{JI}^{\mathrm{T}}}_{\bar{\boldsymbol{w}}_J^{\mathrm{T}}}]^{\mathrm{T}}, \tag{13}$$

where $\bar{\boldsymbol{w}}$ is the reshaped vector by reordering $\boldsymbol{w}$ with respect to output channels, and $\bar{\boldsymbol{w}}_j$ is the vector containing the filter coefficients of the $j$-th output channel. However, the constraint in (11) is non-convex and discontinuous, which brings serious challenges for problem-solving.

### B. Problem Reformulation

We first relax the constraint in (11) using the complete square inequality

$$I_w J_w = \|\boldsymbol{w}\|_{0,2}\|\bar{\boldsymbol{w}}\|_{0,2} \leq \frac{1}{2}(\|\boldsymbol{w}\|_{0,2}^2 + \|\bar{\boldsymbol{w}}\|_{0,2}^2). \tag{14}$$

Building on this, we reformulate the problem (11) by exchanging its constraint and objective. This involves minimizing the group sparsity of the filter coefficients while constraining the residual noise power with a lower bound $\alpha$, i.e.,

$$\begin{aligned} \min_{\boldsymbol{w}} \quad & \|\boldsymbol{w}\|_{0,2}^2 + \|\bar{\boldsymbol{w}}\|_{0,2}^2 \\ \text{subject to} \quad & \hat{d} + 2\boldsymbol{w}^{\mathrm{T}}\boldsymbol{g} + \boldsymbol{w}^{\mathrm{T}}\boldsymbol{H}\boldsymbol{w} \leq \alpha. \end{aligned} \tag{15}$$

Note that (15) is equivalent to (11) after determining an appropriate $\alpha$. However, the $\ell_{0,2}$-norm in (15) is non-convex. Inspired by [18], [19], the $\ell_{0,2}$-norm can be replaced with the $\ell_{1,2}$-norm (by substituting the $\ell_0$-norm in (12) with the $\ell_1$-norm), then (15) can be reformulated as

$$\begin{aligned} \min_{\boldsymbol{w}} \quad & \mathbf{1}_I^{\mathrm{T}}\boldsymbol{p} + \mathbf{1}_J^{\mathrm{T}}\boldsymbol{q} \\ \text{subject to} \quad & \hat{d} + 2\boldsymbol{w}^{\mathrm{T}}\boldsymbol{g} + \boldsymbol{w}^{\mathrm{T}}\boldsymbol{H}\boldsymbol{w} \leq \alpha, \\ & \|\boldsymbol{w}_i\|_2^2 \leq p_i,\ i = 1, \cdots, I, \\ & \|\bar{\boldsymbol{w}}_j\|_2^2 \leq q_j,\ j = 1, \cdots, J, \end{aligned} \tag{16}$$

where $\mathbf{1}_I$ represents the $I$ dimensional column vector with all elements being 1, $\boldsymbol{p} = [p_1, p_2\ \ldots\ p_I]^{\mathrm{T}}$, and $\boldsymbol{q} = [q_1, q_2\ \ldots\ q_J]^{\mathrm{T}}$. This problem can be solved by existing solvers such as CVX [20] or SeDuMi [21]. When $p_i$ or $q_j$ is zero, it is reasonable to put the $i$-th input channel or the $j$-th output channel to sleep during the execution of ANC. In other words, only the selected channels are activated to perform the ANC after solving (16). Furthermore, by observing (16) we can conclude that

- Removing $\boldsymbol{q}$ allows (16) to become an input channel selection (ICS) problem, from which the optimal subset of input channels can be determined when activating all output channels;
- By removing $\boldsymbol{p}$, (16) degenerates into an output channel selection (OCS) problem, from which the optimal subset of output channels can be determined when activating all input channels;
- By directly solving (16), we can obtain the optimal combination of input and output channels. Compared to ICS and OCS, it can simultaneously reduce redundancy in both input and output channels, thus delivering higher computational efficiency.

As we mentioned earlier, (16) is equivalent to (11) as long as finding an appropriate $\alpha$. To this end, we will propose a computation rule of $\alpha$ in the next subsection.

### C. Computation Rule of $\alpha$

To determine an appropriate $\alpha$ that satisfies the constraint in (11), we propose a computing rule based on bisection searching. Since $\alpha$ in (16) represents the predefined residual noise power, the bisection searching interval, i.e., $[\alpha_{Min}, \alpha_{Max}]$, can be initialized by the residual noise power in (9) when activating all input and output channels or turning off the ANC controller. The detailed iterative procedure is described in Algorithm 1, where $t$ denotes the index of bisection searching iterations and $c$ refers to the right-hand side of the constraint in (11), i.e., $c = \frac{B_0-K}{K(L+M)+M}$.

The termination condition in Algorithm 1 requires that $I_w(t)J_w(t) \leq c$ and $(I_w(t)+1)J_w(t) > c \cup I_w(t)(J_w(t)+$

$1) > c$ should be satisfied at the same time. The first term $I_w(t)J_w(t) \leq c$ is coincident with the constraint in (11), while the second term $(I_w(t)+1)J_w(t) > c \cup I_w(t)(J_w(t)+1) > c$ allows the inequality constraint $I_w(t)J_w(t) \leq c$ as close as possible to an equality to pursue the maximum ANC performance. At this point, (16) and (11) possess approximate solutions.

**Algorithm 1** Computate $\alpha$ based on bisection searching

**input :** $c, \hat{d}, \boldsymbol{g}, \boldsymbol{H}, \alpha_{Min}(0), \alpha_{Max}(0)$
**output:** $\alpha(t)$

```
repeat
    α(t) = (α_Max(t − 1) + α_Min(t − 1))/2;
    Solve (16) with α(t) to obtain I_w(t) and J_w(t);
    if I_w(t)J_w(t) ≤ c then
        α_Max(t) = α(t);
    else
        α_Min(t) = α(t);
    end
until {I_w(t)J_w(t) ≤ c} ∩ {(I_w(t) + 1)J_w(t) > c ∪ I_w(t)(J_w(t) + 1) > c};
```

## IV. Simulation Result

The simulation environment was an enclosure of size $3\,\mathrm{m} \times 3\,\mathrm{m}$, where 2 noise sources, 10 RMs, 6 loudspeakers, and 3 EMs were randomly distributed (Fig. 2). Two noise sources played real recorded noises from dataset [22]. The sampling rate was set to 16 kHz, and the signal length $N$ for selection was set to 48000 samples. When selecting all channels, the computational load $B = 10503$. The step size and the filter order were fixed to $\mu = 1.0 \times 10^{-7}$ and $M = L = 25$, respectively.

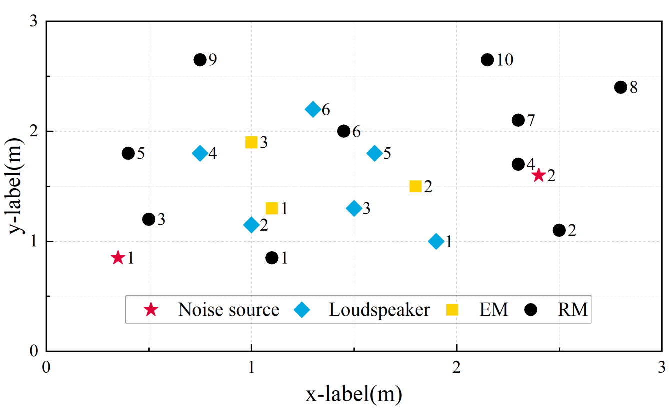


Fig. 2. Geometry configuration, including 2 noise sources, 10 RMs, 6 loudspeakers, and 3 EMs in an enclosure.

In the subsequent experiments, we used the normalized mean squared error (NMSE) as the evaluation metric, which is defined by

$$\mathrm{NMSE} = 10 \log_{10} \frac{\sum_{n=1}^{N_{lms}} \sum_{k=1}^{K} e_k^2(n)}{\sum_{n=1}^{N_{lms}} \sum_{k=1}^{K} \hat{d}_k^2(n)}, \tag{17}$$

where $N_{lms}$ represents the signal length during MEFxLMS filtering, which is set to $N_{lms} = 160000$ samples. Obviously, the lower the NMSE, the better the noise reduction effect.

### A. Effectiveness of Joint Input and Output Channel Selection

We first evaluated the effectiveness of the joint input and output channel selection (J-IO-CS) after setting the upper bound $B_0$ of computational load to $B_0 = 5500$. As discussed below (16), we also conducted the input channel selection (ICS) and the output channel selection (OCS) by removing $\boldsymbol{q}$ and $\boldsymbol{p}$ from (16).

Fig. 3 shows the comparison results of three selection strategies. The ICS selects input channels {1, 3, 4, 5, 8} while activating all output channels; the OCS selects output channels {2, 3, 5} while activating all input channels; and the J-IO-CS selects input channels {1, 3, 4, 5, 8, 10} and output channels {2, 3, 4, 5, 6}. As depicted in Fig. 3, the overall NMSE (red bar) of the J-IO-CS is significantly lower than that of the other two methods, demonstrating the effectiveness of joint input and output channel selection. This is because the J-IO-CS can reduce the redundancy within both input and output channels. To be specific, the NMSE of the J-IO-CS is comparable to that of OCS at EM {1}, both of them perform better than ICS; all three methods provide similar NMSEs at EM {2}; and the J-IO-CS performs best at EM {3}.

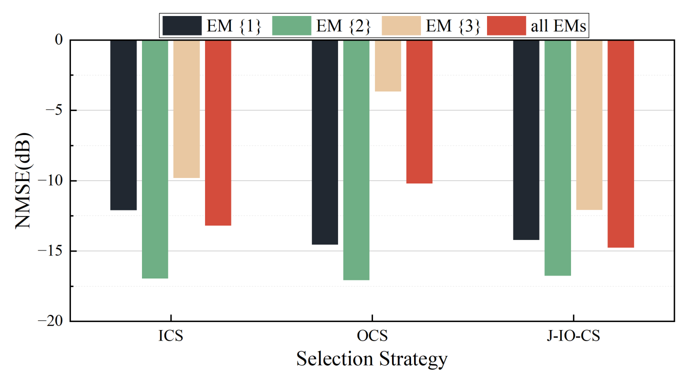


Fig. 3. Noise reduction performance of three different selection strategies under the same computational complexity.

### B. Performance under Different Computational Complexities

In this part, we further tested the details of the J-IO-CS method by specifying different computational complexities, i.e., $B_0 = \{1000, 3000, 5000, 7000, 9000\}$. As shown in Table I, the actual computational complexity $B_s$ after channel selection is always less than and close to the pre-defined upper bound $B_0$. The reason is that the proposed computation rule of $\alpha$ allows the reformulated problem (16) to be approximated to the original problem (11). In addition, the number of input and output channels gradually increases as $B_0$ increases, leading to improved noise reduction performance. Moreover, it is evident that the decrease in NMSE rate becomes smaller with raising $B_0$, due to the fact that redundancy in channels increases as the number of channels increases. This phenomenon further emphasizes the necessity of selecting the input and output channels. It can also be seen that the bisection searching converges within at least 6 iterations. We would like to note that all channels can be activated to conduct multi-channel

TABLE I
SELECTION BASED ON DIFFERENT UPPER BOUND $B_0$ OF COMPUTATIONAL LOAD.

| $B_0$ <br> $B_s$ | 1000 <br> 703 | 3000 <br> 2628 | 5000 <br> 4378 | 7000 <br> 6302 | 9000 <br> 8403 |
|---|---|---|---|---|---|
| Selected input channels | {3,4} | {1,3,4} | {1,3,4, 5,8} | {1,3,4, 5,8,10} | {1,2,3,4, 5,7,8,10} |
| Selected output channels | {2,5} | {2,3,4, 5,6} | {2,3,4, 5,6} | {1,2,3, 4,5,6} | {1,2,3, 4,5,6} |
| NMSE(dB) | -4.41 | -7.34 | -12.99 | -14.98 | -15.83 |
| num. of iter. | 4 | 3 | 4 | 6 | 5 |

feedforward ANC before obtaining the channel selection results using the proposed method.

### C. Comparison Experiment

To the best of our knowledge, the J-IO-CS is the first attempt to simultaneously select input and output channels in multi-channel feedforward ANC systems, thus only existing input channel selection methods, i.e., the CWD [15] and the causality-constraint-based selection (CCS) [13], were carried out to act as the baselines. All methods were executed multiple times with different numbers of activated channels to evaluate the computational efficiency of the multi-channel feedforward ANC system. As shown in Fig. 4, it can be observed that the NMSE of the J-IO-CS is always lower than that of the other two methods. The reason is twofold: the designed channel selection criterion outperforms existing rules based on coherence [15] or causality [13]; the joint selection of input and output channels is superior to selecting only input channels.

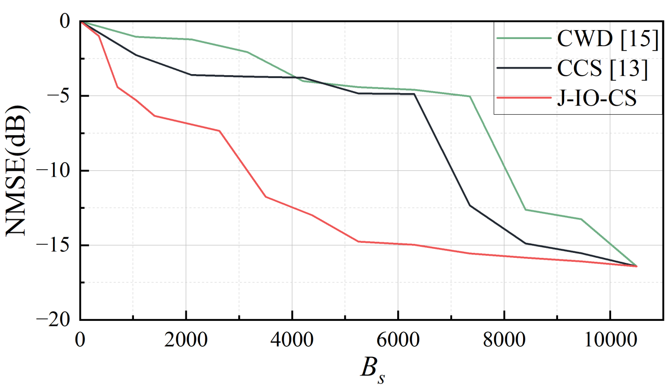


Fig. 4. Computational efficiency evaluation.

## V. CONCLUSION

This paper proposed a joint input and output channel selection (J-IO-CS) method for multi-channel feedforward ANC to improve the system's computational efficiency. It was achieved by promoting the group sparsity of the spatial filter after constraining the ANC performance. Furthermore, the proposed method can also be driven by a constraint of computational complexity by seeking a suitable ANC performance constraint. The simulation results confirmed its effectiveness. In our future work, we will study how to combine the J-IO-CS with filter-order determination to further improve computational efficiency.

## REFERENCES

[1] T. Watanabe, S. Kanai, and T. Atsumi, "Effects of wind noise on hybrid active noise cancellation headphones," in *Proc. IEEE Int. Conf. Ind. Technol.*, Orlando, FL, USA, 2023, pp. 1–6.
[2] S. Bagha, D. P. Das, and S. K. Behera, "Reference microphone free active headrest system for noise containing varying frequency tonal components," *IEEE Trans. Circuits Syst. II: Exp. Briefs*, pp. 3184 – 3188, Aug. 2023.
[3] J. Y. Oh, H. W. Jung, M. H. Lee, K. H. Lee, and Y. J. Kang, "Enhancing active noise control of road noise using deep neural network to update secondary path estimate in real time," *Mech. Syst. Signal Process.*, vol. 206, p. 110940, Jan. 2024.
[4] S. M. Kuo and D. R. Morgan, "Active noise control: A tutorial review," *Proc. IEEE*, vol. 87, no. 6, pp. 943–973, Jun. 1999.
[5] S. J. Elliott and P. A. Nelson, "Active noise control," *IEEE Signal Process. Mag.*, vol. 10, no. 4, pp. 12–35, Oct. 1993.
[6] B. Lam, W.-S. Gan, D. Shi, M. Nishimura, and S. Elliott, "Ten questions concerning active noise control in the built environment," *Build. Environ.*, vol. 200, p. 107928, Aug. 2021.
[7] D. Shi, B. Lam, J. Ji, X. Shen, C. K. Lai, and W.-S. Gan, "Computation-efficient solution for fully-connected active noise control window: Analysis and implementation of multichannel adjoint least mean square algorithm," *Mech. Syst. Signal Process.*, vol. 199, p. 110444, Sep. 2023.
[8] S. Elliott, *Signal Processing for Active Control*. Academic Press, 2001.
[9] S. Hase, Y. Kajikawa, L. Liu, and S. M. Kuo, "Multi-channel ANC system using optimized reference microphones based on time difference of arrival," in *Proc. IEEE 23rd Eur. Signal Process. Conf.*, Nice, France, 2015, pp. 305–309.
[10] M. L. N. S. Karthik, S. Joel, and N. V. George, "FxLMS/F based tap decomposed adaptive filter for decentralized active noise control system," *IEEE/ACM Trans. Audio, Speech, Lang. Process.*, vol. 32, pp. 4691–4699, Oct. 2024.
[11] C. Shi and Y. Kajikawa, "A partial-update minimax algorithm for practical implementation of multi-channel feedforward active noise control," in *Proc. 16th Int. Workshop Acoust. Signal Enhanc.*, Tokyo, Japan, 2018, pp. 1–15.
[12] S. M. Kuo and D. R. Morgan, *Active Noise Control Systems*, New York, NY, USA: Wiley, vol. 4, 1996.
[13] K. Iwai, S. Hase, and Y. Kajikawa, "Multichannel feedforward active noise control system with optimal reference microphone selector based on time difference of arrival," *Appl. Sci.*, vol. 8, no. 11, pp. 1–17, Nov. 2018.
[14] J. A. Zhang, N. Murata, Y. Maeno, P. N. Samarasinghe, T. D. Abhayapala, and Y. Mitsufuji, "Coherence-based performance analysis on noise reduction in multichannel active noise control systems," *J. Acoustical Soc. Amer.*, vol. 148, no. 3, pp. 1519–1528, Sep. 2020.
[15] X. Shen, D. Shi, S. Peksi, and W.-S. Gan, "A multi-channel wireless active noise control headphone with coherence-based weight determination algorithm," *J. Signal Process. Syst.*, vol. 94, no. 8, pp. 811–819, Mar. 2022.
[16] L. J. Eriksson and M. C. Allie, "Use of random noise for on-line transducer modeling in an adaptive active attenuation system," *J. Acoustical Soc. Amer.*, vol. 85, no. 2, pp. 797–802, Feb. 1989.
[17] S. Elliott, I. Stothers, and P. Nelson, "A multiple error lms algorithm and its application to the active control of sound and vibration," *IEEE Trans. Acoust. Speech Sig. Process.*, vol. 35, no. 10, pp. 1423–1434, Oct. 1987.
[18] E. J. Candès, J. Romberg, and T. Tao, "Robust uncertainty principles: Exact signal reconstruction from highly incomplete frequency information," *IEEE Trans. Inf. Theory*, vol. 52, no. 2, pp. 489–509, Jan. 2006.
[19] M. B. Hawes and W. Liu, "Sparse microphone array design for wideband beamforming," in *Proc. 18th Int. Conf. Digit. Signal Process.*, Fira, Greece, 2013, pp. 1–5.
[20] M. Grant, S. Boyd, and Y. Ye, "CVX: Matlab software for disciplined convex programming," 2008.
[21] J. F. Sturm, "Using SeDuMi: A Matlab toolbox for optimization over symmetric cones," *Optim. Methods Softw.*, vol. 11, no. 1-4, pp. 625–653, Aug. 1999.
[22] C. K. Reddy, E. Beyrami, J. Pool, R. Cutler, S. Srinivasan, and J. Gehrke, "A scalable noisy speech dataset and online subjective test framework," in *Proc. Interspeech 2019*, Graz, Austria, 2019, pp. 1816–1820.